What are Marine Ecological Time Series telling us about the ocean? A status report

[Individual Chapter (PDF) download]

The full report (all chapters and Annex) is available online at:

http://igmets.net/report

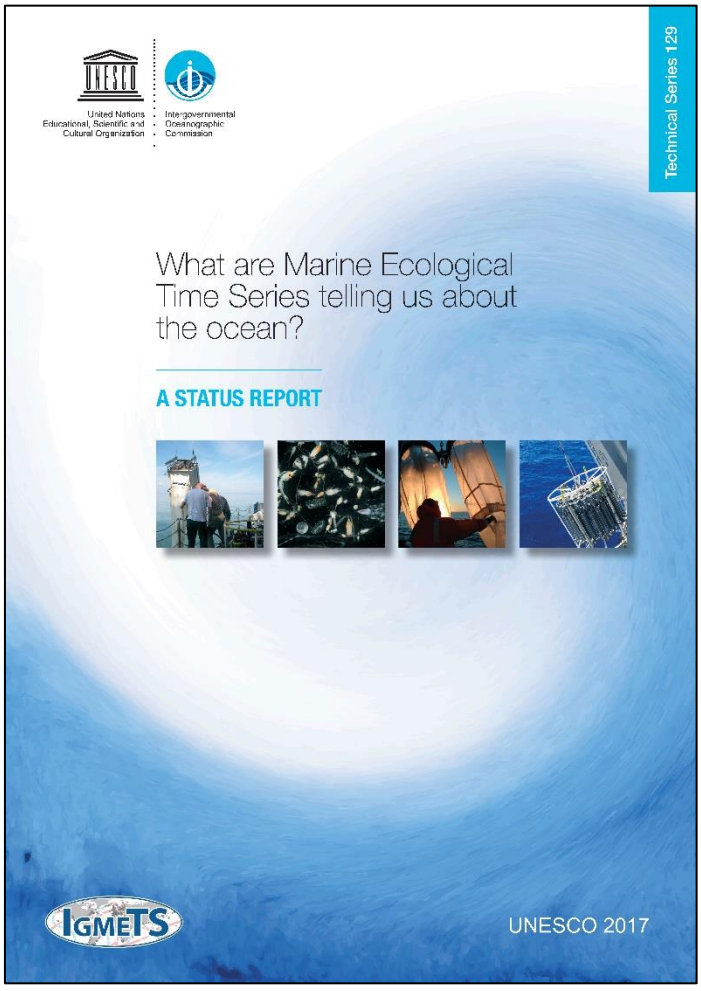

This page intentionally left blank

to preserve pagination in double-sided (booklet) printing

9 North Pacific Ocean

Andrew R. S. Ross, R. Ian Perry, James R. Christian, Todd D. O'Brien, Laura Lorenzoni, Frank E. Muller-Karger, William R. Crawford, Angelica Peña, and Kirsten Isensee

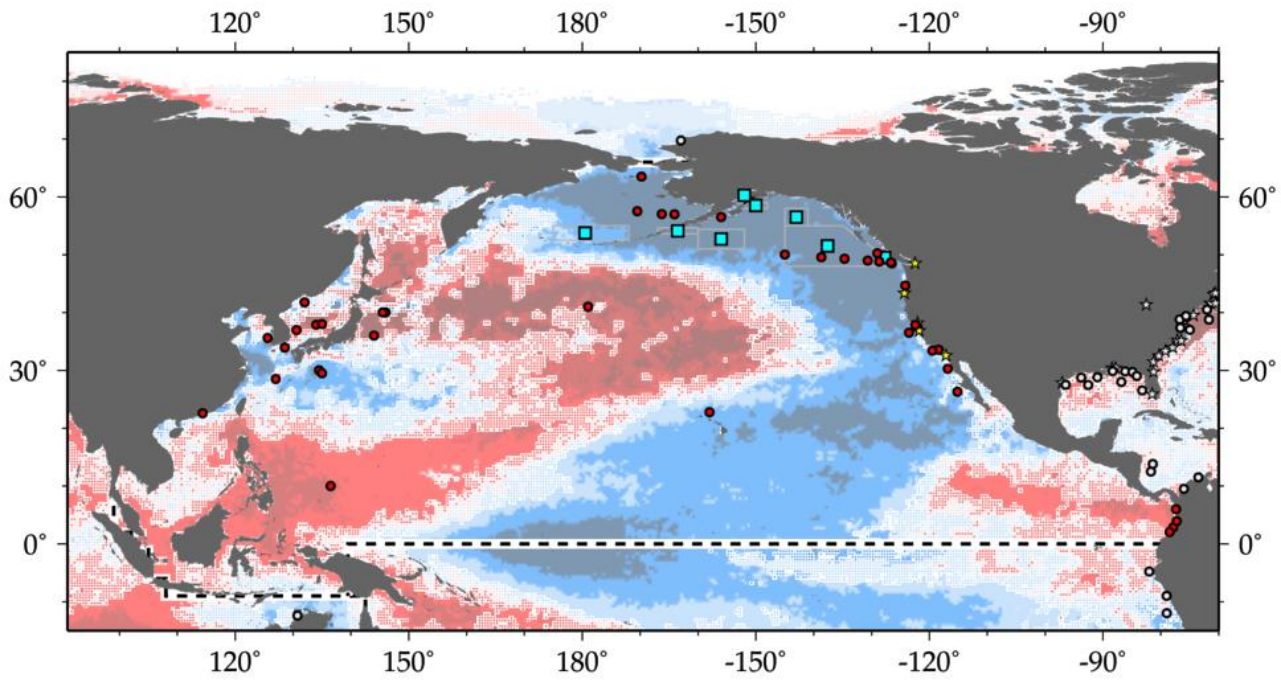

Figure 9.1. Map of IGMETS-participating North Pacific time series on a background of a 10-year time-window (2003–2012) sea surface temperature trends (Figure 9.4). At the time of this report, the North Pacific collection consisted of 54 time series (coloured symbols of any type), of which eight were from Continuous Plankton Recorder subareas (blue boxes), and six were from estuarine areas (yellow stars). Dashed lines indicate boundaries between IGMETS regions. Uncoloured (gray) symbols indicate time series being addressed in a different regional chapter (e.g. Arctic Ocean, South Pacific). See Table 9.3 for a listing of this region's participating sites. Additional information on the sites in this study is presented in the Annex.

Participating time-series investigators

Sonia Batten, Robert Bidigare, David Caron, Sanae Chiba, Matthew J. Church, James E. Cloern, John E. Dore, Janet Duffy-Anderson, Lisa Eisner, Luisa Espinosa, Ed Farley, Jennifer L. Fisher, Jed Fuhrman, Moira Galbraith, Troy Gunderson, Masao Ishii, Young-Shil Kang, David M. Karl, Diane Kim, Michael Landry, Bertha E. Lavaniegos, Ricardo M. Letelier, Roger Lukas, Dave Mackas, Roberta Marinelli, Sam McClatchie, Cheryl A. Morgan, Jeffrey Napp, Todd O'Brien, Mark Ohman, Ian Perry, William T. Peterson, Al Pleudemann, Dwayne Porter, Marie Robert, Andrew R.S. Ross, Sei-ichi Saitoh, Robert Weller, and Kedong Yin

This chapter should be cited as: Ross, A. R. S., Perry, R. I., Christian, J. R., O'Brien, T. D., Lorenzoni, L., Muller-Karger, F. E., Crawford, W. R., *et al.* 2017. North Pacific. I*n* What are Marine Ecological Time Series telling us about the ocean? A status report, pp. 153–169. Ed. by T. D. O'Brien, L. Lorenzoni, K. Isensee, and L. Valdés. IOC-UNESCO, IOC Technical Series, No. 129. 297 pp.

9.1 Introduction

The North Pacific (Figure 9.1) covers an area equivalent to just over one-fifth of the surface of the world's oceans (85 million km^2) and accounts for almost one-fourth of their total volume (331 million km^3). It includes the deepest point in the ocean (10.9 km in the Marianas Trench) and has the greatest average depth (4.3 km) of any ocean basin (Eakins and Sharman, 2010). The North Pacific consists of a large central oceanic region surrounded by a number of boundary currents and marginal seas (McKinnell and Dagg, 2010). These include the Alaska Stream and currents in the Bering Sea that link the Pacific with the Arctic Ocean. They also include the North Equatorial Current, the California Current and Alaska Current to the east, and the Oyashio Current, Kuroshio Current, Sea of Okhotsk, Sea of Japan/East Sea, and Yellow and East China seas to the west. The oceanic region contains a large subtropical gyre to the south and a smaller subarctic gyre to the north, divided by the North Pacific Current.

Pacific Ocean currents (Figure 9.2) follow the general pattern of those in the Atlantic (Bowditch, 2002), although the greater size and semi-enclosed boundaries of the Pacific result in circulation patterns that respond more ideally to the Coriolis effect and symmetrical wind patterns in the two hemispheres (Longhurst, 2007). The North Equatorial Current is driven westward by trade winds before turning north near the Philippines to become the warm Kuroshio Current, which joins the cool southward Oyashio Current to form the eastward Kuroshio–Oyashio Extension (KOE) and North Pacific Current. Western boundary currents like the Kuroshio and the North Atlantic Gulf Stream play an important role in climate change, acting as "hot spots" where the thermodynamic effects of the ocean on the atmosphere are intensified (Minobe *et al.*, 2008; Wu *et al.*, 2012). Changes in the position of the Kuroshio Current and the large meanders that form in this current also affect marine ecology and navigation in the western boundary region (McKinnell and Dagg, 2010). The KOE and North Pacific Current mark the northern boundary of the North Pacific Subtropical Gyre, the largest ecosystem in the surface ocean (Karl, 1999). The Alaska Current, which becomes the Alaska Stream after turning southwest along the Alaskan Peninsular, forms part of the anticlockwise Alaska Gyre and produces large clockwise mesoscale eddies west of Sitka and Haida Gwaii (formerly the Queen Charlotte Islands) that propagate westward into the gyre. Haida eddies play an important role in the offshore transport of zooplankton (Batten and Crawford, 2005) and iron (Johnson *et al.*, 2005) to the high-

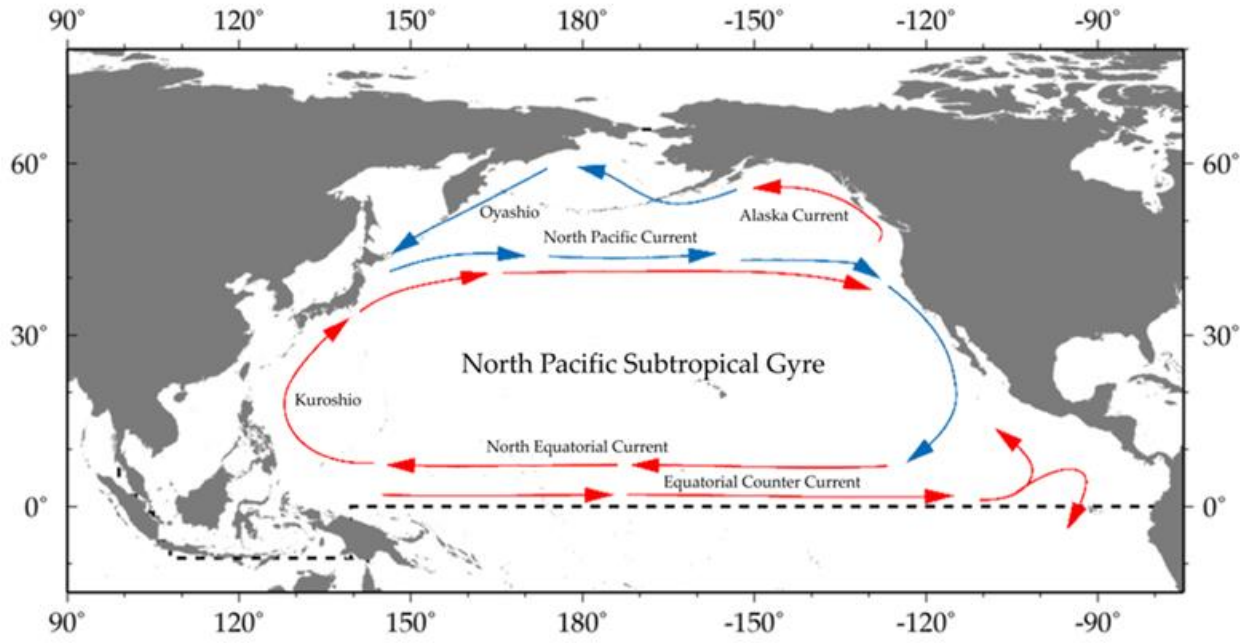

Figure 9.2. Schematic major current systems in the IGMETS-defined North Pacific region. Red arrows indicate generally warmer water currents; blue arrows indicate generally cooler water currents.

nutrient/low-chlorophyll waters of the subarctic Northeast Pacific. Water from the Alaska Current also enters the Bering Sea, forming part of the anticlockwise Bering Sea Gyre. Some of this water flows south into the Oyashio Current, which together with the Alaska Stream forms part of the anticlockwise Western Subarctic Gyre as it turns east to join the North Pacific Current, completing the North Pacific Subarctic Gyre. Water from the Alaska Current also drifts north through the Bering Strait into the Chukchi Sea, contributing to the circulation of the Arctic Ocean (Chapter 3).

The North Pacific lies at the end of the "ocean conveyor belt" (Zenk, 2001) where cold, nutrient-rich, deep water originating from the North Atlantic and Southern Ocean flows northward across the equator (Bowditch, 2002). Upwelling along the eastern boundary of the North Pacific supports high levels of productivity in the coastal waters of western Canada and the United States (McKinnell and Dagg, 2010), but also contributes to the local impacts of ocean acidification, due to the high amounts of dissolved inorganic carbon that accumulate in subsurface waters (Feely *et al.*, 2008; Haigh *et al.*, 2015).

The climate of the North Pacific is characterized by strong interdecadal variability, which arises from modulation of the El Niño–Southern Oscillation (ENSO) signal by the Aleutian Low (AL) and North Pacific Oscillation (NPO). These major atmospheric systems drive two predominant ocean modes: the Pacific Decadal Oscillation (PDO) and the North Pacific Gyre Oscillation (NPGO), respectively (Figure 9.3). The resulting variability gives rise to distinct physical and biological responses in the North Pacific (McKinnell and Dagg, 2010; Di Lorenzo *et al.*, 2013). The Oceanic Niño Index (ONI) is a measure of the anomaly of ocean surface temperature in the east-central equatorial Pacific (Figure 9.3) and defines the occurrence of El Niño and La Niña episodes (http://www.cpc.ncep.noaa.gov/products/analysis_monitoring/ensostuff/ensoyears.shtml). The North Pacific Index (NPI) is the area-weighted sea level pressure over part of the North Pacific and is a useful indicator of the intensity and areal extent of the Aleutian Low (Wallace and Gutzler, 1981; Trenberth and Hurrell, 1994). The PDO is the first mode of ocean surface temperature variability in the North Pacific (Mantua *et al.*, 1997; Zhang *et al.*, 1997) and is often positive during El Niño years (Figure 9.3). PDO variability is slower than that of the ONI and it is usually a good indicator of temperature

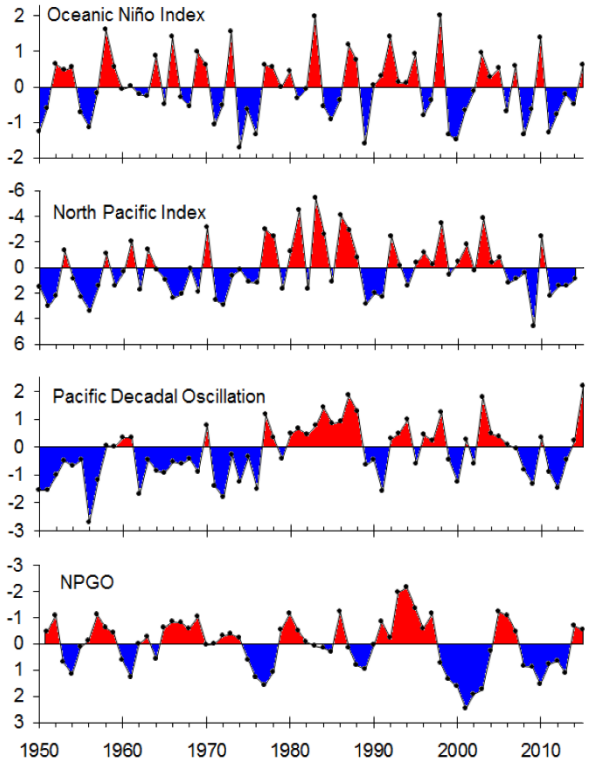

Figure 9.3. North Pacific climate indices, November–March averages (Chandler *et al.*, 2015).

patterns that persist for a decade or more. The NPGO is the second dominant mode of sea surface height variability in the Northeast Pacific and closely tracks the second mode of North Pacific SST (Di Lorenzo *et al.*, 2008). NPGO dynamics are driven by atmospheric variability in the North Pacific and capture the extratropical influence of central Pacific El Niños. When the NPGO is positive, the westerly winds over the eastern North Pacific are often stronger than normal, and the west coast of North America and eastern Gulf of Alaska are cool. These conditions have dominated in most winters from 1999 to 2013, except between 2004 and 2007 (Figure 9.3). The AL/PDO system describes many of the ecosystem fluctuations in the North Pacific (Di Lorenzo *et al.*, 2009). However, long-term time series like CalCOFI (us-50301/2) and Line-P (ca-50901) show decadal-scale fluctuations that are apparently unconnected with the PDO. The NPGO, which is associated with changes in the strength of the subtropical and subarctic gyres, explains the dominant interdecadal fluctuations in salinity, nutrient upwelling, and chlorophyll in many regions of the Northeast Pacific (Di Lorenzo *et al.*, 2009) as well as important state transitions in marine ecosystems (Cloern *et al.*, 2010; Perry and Masson, 2013).

Table 9.1. Relative spatial areas (% of the total region) and rates of change within the North Pacific region that are showing increasing or decreasing trends in sea surface temperature (SST) for each of the standard IGMETS time-windows. Numbers in brackets indicate the % area with significant ($p < 0.05$) trends. See "Methods" chapter for a complete description and methodology used.

Latitude-adjusted SST data field surface area = 85.4 million km²	**5-year** (2008–2012)	**10-year** (2003–2012)	**15-year** (1998–2012)	**20-year** (1993–2012)	**25-year** (1988–2012)	**30-year** (1983–2012)
Area (%) w/ increasing SST trends ($p < 0.05$)	42.8% (*7.9%*)	44.6% (*26.4%*)	**65.3%** (*41.8%*)	**65.0%** (*49.1%*)	**67.9%** (*56.5%*)	**75.7%** (*64.7%*)
Area (%) w/ decreasing SST trends ($p < 0.05$)	**57.2%** (*19.9%*)	**55.4%** (*41.4%*)	34.7% (*18.9%*)	35.0% (*24.1%*)	32.1% (*21.3%*)	24.3% (*16.8%*)
> 1.0°C decade^{-1} warming ($p < 0.05$)	9.2% (*4.9%*)	3.8% (*3.8%*)	0.8% (*0.8%*)	0.1% (*0.1%*)	0.0% (*0.0%*)	0.0% (*0.0%*)
0.5 to 1.0°C decade^{-1} warming ($p < 0.05$)	10.7% (*2.4%*)	10.0% (*9.1%*)	6.0% (*5.9%*)	6.5% (*6.5%*)	0.7% (*0.7%*)	1.8% (*1.8%*)
0.1 to 0.5°C decade^{-1} warming ($p < 0.05$)	17.1% (*0.7%*)	24.7% (*13.3%*)	46.6% (*34.4%*)	44.9% (*40.7%*)	**50.6%** (*49.0%*)	**55.4%** (*54.9%*)
0.0 to 0.1°C decade^{-1} warming ($p < 0.05$)	5.8% (*0.0%*)	6.1% (*0.2%*)	11.9% (*0.7%*)	13.6% (*1.9%*)	16.6% (*6.8%*)	18.6% (*8.0%*)
0.0 to –0.1°C decade^{-1} cooling ($p < 0.05$)	5.6% (*0.0%*)	5.0% (*0.1%*)	9.1% (*0.3%*)	8.1% (*0.5%*)	11.6% (*1.9%*)	9.9% (*2.8%*)
–0.1 to –0.5°C decade^{-1} cooling ($p < 0.05$)	18.3% (*0.5%*)	16.6% (*7.9%*)	20.8% (*13.8%*)	22.6% (*19.3%*)	20.4% (*19.2%*)	14.3% (*14.1%*)
–0.5 to –1.0°C decade^{-1} cooling ($p < 0.05$)	13.5% (*3.9%*)	22.2% (*21.8%*)	4.4% (*4.4%*)	4.3% (*4.3%*)	0.1% (*0.1%*)	0.0% (*0.0%*)
> –1.0°C decade^{-1} cooling ($p < 0.05$)	19.8% (*15.4%*)	11.5% (*11.5%*)	0.4% (*0.4%*)	0.0% (*0.0%*)	0.0% (*0.0%*)	0.0% (*0.0%*)

Table 9.2. Relative spatial areas (% of the total region) and rates of change within the North Pacific region that are showing increasing or decreasing trends in phytoplankton biomass (CHL) for each of the standard IGMETS time-windows. Numbers in brackets indicate the % area with significant ($p < 0.05$) trends. See "Methods" chapter for a complete description and methodology used.

Latitude-adjusted CHL data field surface area = 85.4 million km²	**5-year** (2008–2012)	**10-year** (2003–2012)	**15-year** (1998–2012)
Area (%) w/ increasing CHL trends ($p < 0.05$)	23.6% (*2.9%*)	40.8% (*21.2%*)	34.2% (*13.0%*)
Area (%) w/ decreasing CHL trends ($p < 0.05$)	**76.4%** (*35.8%*)	**59.2%** (*37.3%*)	**65.8%** (*42.7%*)
> 0.50 mg m^{-3} decade^{-1} increasing ($p < 0.05$)	0.9% (*0.3%*)	0.3% (*0.3%*)	0.6% (*0.5%*)
0.10 to 0.50 mg m^{-3} decade^{-1} increasing ($p < 0.05$)	2.9% (*0.5%*)	3.2% (*1.9%*)	4.0% (*3.3%*)
0.01 to 0.10 mg m^{-3} decade^{-1} increasing ($p < 0.05$)	11.8% (*1.9%*)	25.2% (*16.3%*)	15.4% (*8.0%*)
0.00 to 0.01 mg m^{-3} decade^{-1} increasing ($p < 0.05$)	8.0% (*0.2%*)	12.0% (*2.9%*)	14.2% (*1.2%*)
0.00 to –0.01 mg m^{-3} decade^{-1} decreasing ($p < 0.05$)	11.6% (*1.1%*)	16.7% (*6.7%*)	37.5% (*21.9%*)
–0.01 to –0.10 mg m^{-3} decade^{-1} decreasing ($p < 0.05$)	47.7% (*23.7%*)	39.2% (*28.6%*)	27.5% (*20.4%*)
–0.10 to –0.50 mg m^{-3} decade^{-1} (decreasing) ($p < 0.05$)	14.8% (*9.7%*)	2.9% (*1.7%*)	0.7% (*0.4%*)
> –0.50 mg m^{-3} decade^{-1} (decreasing) ($p < 0.05$)	2.3% (*1.3%*)	0.3% (*0.2%*)	0.1% (*0.1%*)

The following describes the main patterns observed from 1983 to 2012 in North Pacific time-series data compiled by IGMETS and how these relate to known ocean circulation patterns, climate drivers, and previous reports regarding the spatial and temporal variability of marine ecosystems in this region. More detailed tables and maps for the North Pacific and other regions can be obtained from the IGMETS Explorer tool:

http://igmets.net/explorer/

9.2 General patterns of temperature and phytoplankton biomass

Time series of gridded, large-scale, satellite-derived sea surface temperature (SST) and surface chlorophyll (CHL) indicate a general warming accompanied by an overall decrease in phytoplankton biomass in the North Pacific (Tables 9.1 and 9.2). During the 30 years from 1983 to 2012, >75% of the North Pacific (64.7% at $p < 0.05$) underwent warming, whereas 24.3% (16.8% at $p < 0.05$) underwent cooling. The pattern of warming resembles the characteristic "wedge and horseshoe" configuration of the PDO, which is the dominant mode of variability at this time-scale, along with the underlying anthropogenic (secular) trend (Figure 9.4a). During the 15 years from 1998 to 2012, about 35% (18.9% at $p < 0.05$) of North Pacific surface water underwent cooling and 65.3% (41.8% at $p < 0.05$) underwent warming (Table 9.1). Cooling occurred primarily in the eastern North Pacific from the Bering Sea and Alaska Gyre to the California Current and across the southeast North Pacific (Figure 9.4a). Cooling of the Kuroshio Current was also apparent during this period, although the observed pattern may also reflect changes in the position of the Kuroshio axis, which is linked to the PDO (Di Lorenzo *et al*., 2013). The onset of these changes appears to coincide with the abrupt shift from El Niño to La Niña conditions in summer 1998.

Satellite-derived surface chlorophyll data are available for the 15 years from 1998 to 2012. During this period, a decrease in chlorophyll was observed in 65.8% (42.7% at $p < 0.05$) of the surface area of the North Pacific (Table 9.2), mainly in the central oceanic region (Figure 9.4b). At the same time, chlorophyll was seen to increase in 34.2% (13% at $p < 0.05$) of the North Pacific, including parts of the North American west coast, eastern subarctic and equatorial Pacific, and coasts of the Okhotsk and Bering seas. During the 10 years from 2003 to 2012, chlorophyll decreased in 59.2% (37.3% at $p < 0.05$) and increased in 40.8% (21.2% at $p < 0.05$) of the North Pacific. This period coincided with significant cooling over 55.4% (41.8% *at* $p < 0.05$) of the ocean's surface (Table 9.1) and with the appearance of a large patch of chlorophyll to the south, aligned roughly with the North Equatorial Current (Figure 9.4b).

A similar patch was observed in the northern South Pacific during the same period (Chapter 8), the divergence of these features in the eastern equatorial Pacific reflecting the symmetry of the prevailing wind patterns and the influence of Ekman transport (Longhurst, 2007). Direct correlation of chlorophyll with SST (Figure 9.4c) shows that warming tends to be associated with lower phytoplankton biomass over much of the North Pacific, except for parts of the western boundary, central subtropical, and subarctic regions. In the western subarctic Pacific, winter mixed layers are deep and, in some seasons, thermal stratification may promote phytoplankton growth by increasing access to light (Dutkiewicz *et al*., 2001).

9.3 Trends from *in situ* time series

The *in situ* time-series datasets available for the North Pacific are fewer in number than for the North Atlantic (Chapter 4), but are relatively well distributed, providing data from the eastern, western, subarctic, and/or subtropical North Pacific, depending on which parameter is selected (Figure 9.5). They include ship-based measurements of SST and chlorophyll which, when superimposed on the corresponding gridded data, show good overall agreement between *in situ* and satellite-based observations (Figure 9.5a). A selection of other *in situ* variables, combined with gridded SST for the 10-year time-window (Figures 9.5b–h), illustrate how local and regional trends in physical, chemical, and biological parameters can be compared and related and how powerful this approach is for understanding trends in the biogeochemistry of the North Pacific. For example, *in situ* measurements of surface nitrate (Figure 9.5b), salinity (Figure 9.5g), and dissolved oxygen (Figure 9.5h) show a general increase in the eastern and subarctic North Pacific during the 10-year time-window (2003–2012), whereas SST shows the opposite trend. Conversely, in the western North Pacific, warmer SST was largely associated with a decrease in surface salinity, nutrients, and oxygen concentrations. The inverse relationship between temperature and nutrients (nitrate, phosphate,

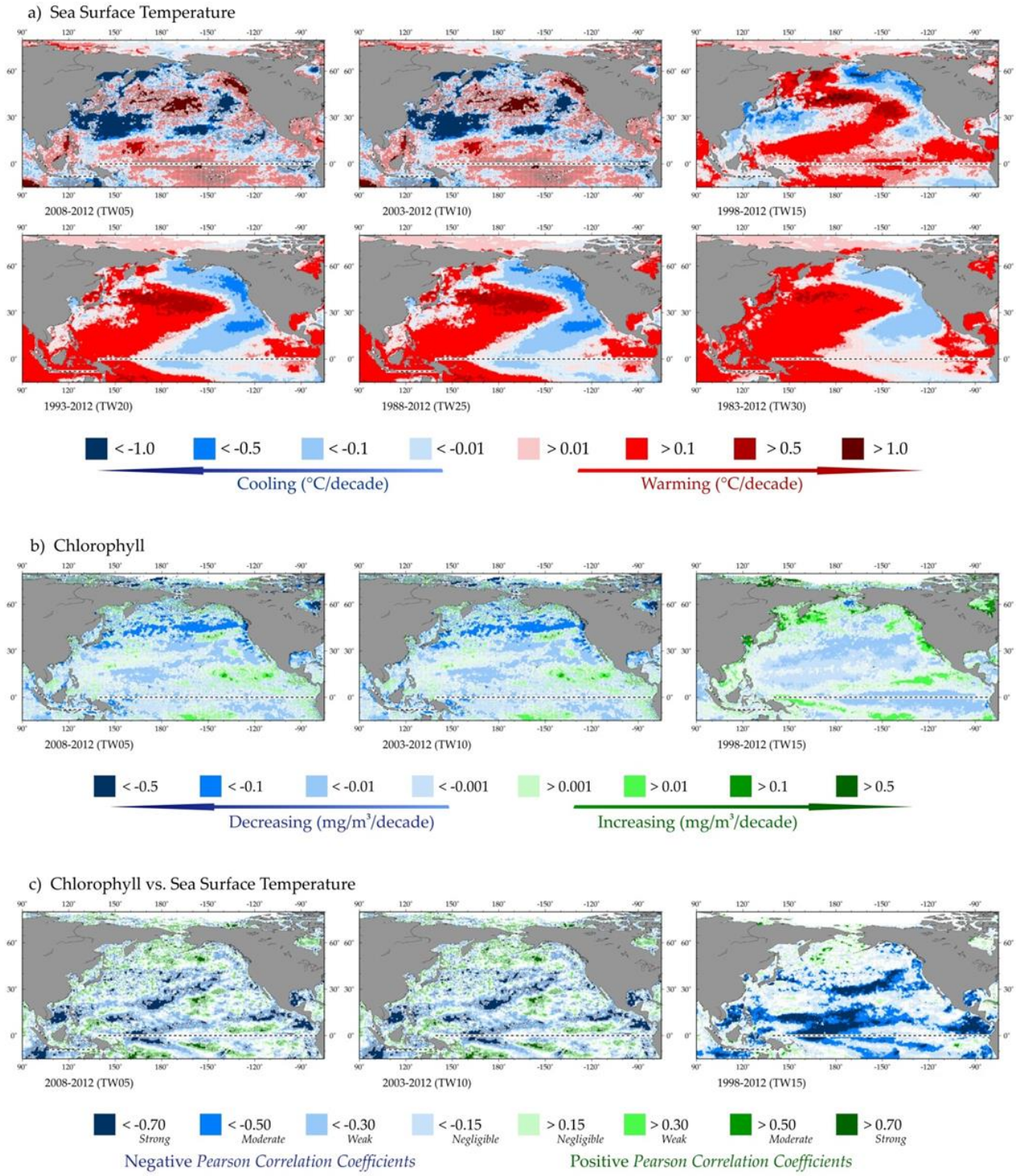

Figure 9.4. Annual trends in North Pacific sea surface temperature (SST) (a) and sea surface chlorophyll (CHL) (b), and correlations between chlorophyll and sea surface temperature for each of the standard IGMETS time-windows (c). See "Methods" chapter for a complete description and methodology used.

and silicate) predominates across the North Pacific over the 30-year time-window (1983–2012) and is consistent with a reduction in the mixing of nutrients into surface waters due to stratification.

Another way of looking at overall trends across the North Pacific is to consider the proportion of available time series that show an increasing or decreasing trend for each *in situ* parameter within a particular time-window. These data can be normalized by expressing them as a percentage of the total number of available sites, making it easier to compare different variables (Figure 9.6). Many of the *in situ* variables in the North Pacific show temporal trends that change in magnitude or direction halfway through the 30-year period from 1983 to 2012, coinciding with the major shift from El Niño to La Niña conditions in 1998 (Figure 9.6c).

For example, the long-term, 30-year trend for *in situ* phytoplankton data is one of increasing chlorophyll (Figure 9.6d), but this trend appears to have slowed since 1998 (Figures 9.6a–c). Considering that most of the *in situ* time series are located in northern and/or coastal waters, with few in tropical or subtropical oceanic waters, these trends are consistent with the assessment of surface chlorophyll based on satellite data (Figure 9.4), which suggests an overall increase in phytoplankton biomass near coastal areas. However, the inclusion of the four equatorial Colombian coastline REDCAM time series (see Table 9.3) contributes to the predominant number of *in situ* measurements showing an increase in temperature between 2008 and 2012 (Figure 9.6a), which contrasts with the overall cooling trend observed in satellite SST across the North Pacific during the same 5-year period (Table 9.1). Neverthless, nitrate time-series measurements show the same inverse relationship with *in situ* temperature (Figure 9.6) as with satellite SST (Figure 9.5b). The available *in situ* data also suggest that zooplankton and diatoms have decreased in most time series during the past 15 years (Figures 7.6a–c). Time series that show increasing chlorophyll are sometimes associated with decreases in zooplankton, especially in the subarctic North Pacific.

Pairwise correlation of *in situ* parameters with Reynolds SST or satellite chlorophyll data allows for an investigation of potential cause-and-effect relationships between these variables. Such a comparison shows synchrony between *in situ* and local gridded SST data (Figure 9.7), but suggests that there is no clear relationship between *in situ* SST and satellite chlorophyll measurements (Figure 9.8), based on the available data. Indeed, there is little correlation between *in situ* parameters and the local gridded chlorophyll data other than an overall positive correlation with nitrate and phytoplankton biomass (Figure 9.8c). In contrast, nitrate, chlorophyll, salinity, and dissolved oxygen time series generally show negative correlations with gridded SST (Figure 9.7). Most phytoplankton time series also showed a negative correlation between the diatom/dinoflagellate ratio and SST (Figure 9.7), as opposed to the positive correlation between this ratio and satellite chlorophyll (Figure 9.8), although the latter is more variable. The majority of zooplankton, diatom, and dinoflagellate time series were positively correlated with SST over the last 10 years (Figure 9.7b). However, it should be born in mind that these basin-scale relationships may not apply at the local or regional level. Furthermore, as mentioned above, the available *in situ* time series cover only a small and mainly peripheral area of the North Pacific, whereas the gridded SST and chlorophyll data cover the entire basin. This, together with the possibility of seasonal effects, may account for apparent discrepancies between *in situ* and satellite-based trends. Increasing time series coverage of the North Pacific would help to address this issue.

9.4 Comparison with other studies

Changing conditions of the North Pacific have been the focus of multiple studies. Fisheries and Oceans Canada (DFO) has been preparing annual State of the Pacific Ocean (SOPO) reports on conditions in the subarctic Northeast Pacific since 1999 (http://www.dfo-mpo.gc.ca/oceans/publications/index-eng.html) using data from oceanic and coastal time series such as the Line-P (ca-50901-6) and offshore Vancouver Island (ca-50301-2) monitoring programmes. Similarly, the North Pacific Marine Science Organization (PICES) has prepared two Special Publications on Marine Ecosystems of the North Pacific Ocean covering the periods 1998–2003 and 2003–2008 (PICES, 2004; McKinnell and Dagg, 2010) using time-series data provided by PICES member nations and participating international organizations such as SAHFOS/Pacific CPR (uk-40201-8). These documents provide a wealth of information on changes in the climate and oceanography of the North Pacific, with which the last 15 years of this IGMETS assessment (1998–2012) can be compared. The first North Pacific Ecosystems

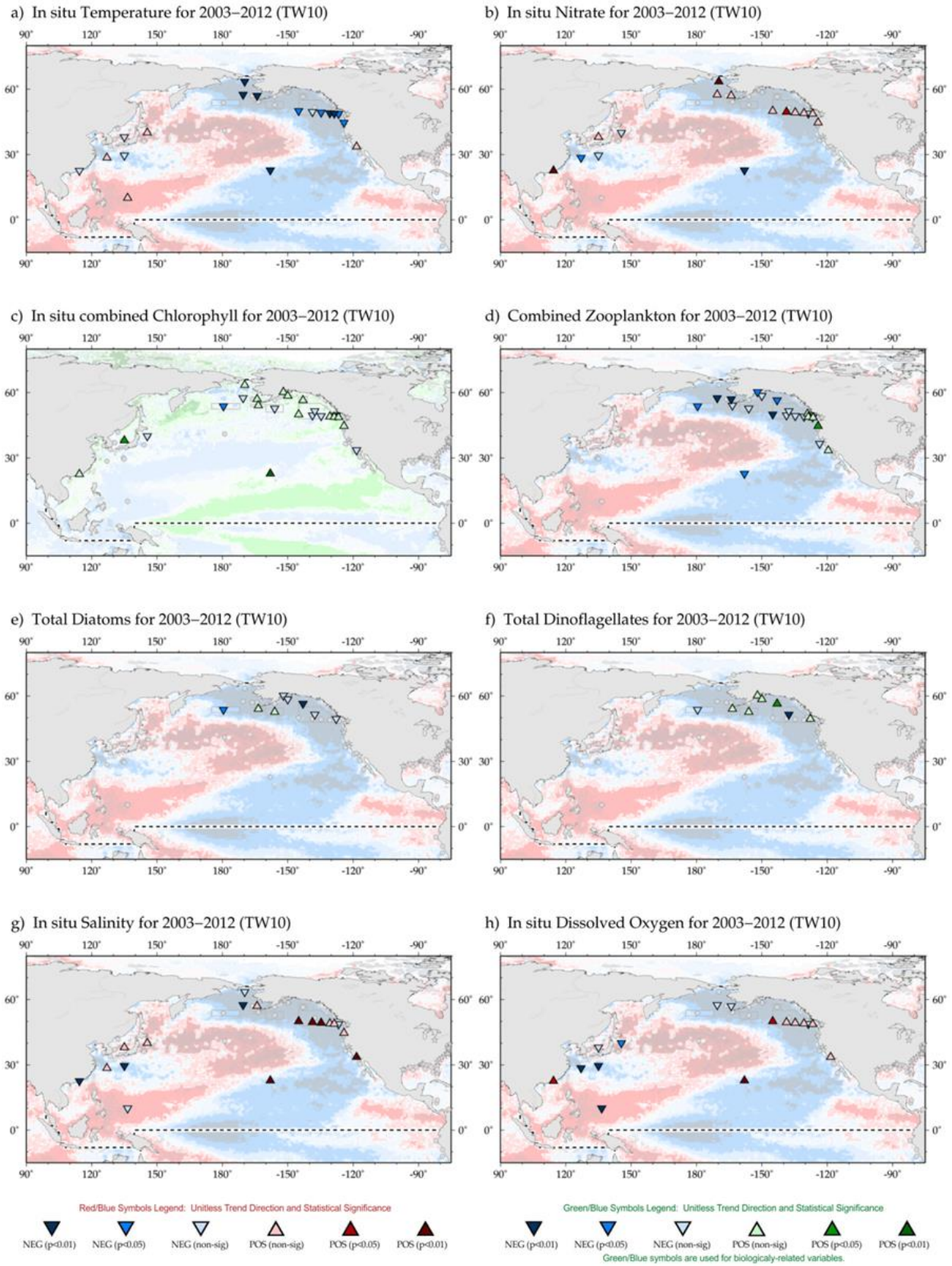

Figure 9.5. Map of North Pacific region time-series locations and trends for select variables and IGMETS time-windows. Upward-pointing triangles indicate positive trends; downward triangles indicate negative trends. Gray circles indicate time-series site that fell outside of the current study region or time-window. Additional variables and time-windows are available through the IGMETS Explorer (http://IGMETS.net/explorer). See "Methods" chapter for a complete description and methodology used.

Status Report (PICES, 2004) describes the emergence of a new climate pattern between 1998 and 2002 associated with a cooling along the eastern boundary and warming of the central North Pacific. SOPO reports for this period (DFO, 2000–2002) describe a return to relatively normal conditions of temperature and plankton ecology following the El Niño/La Niña transition in 1998, although the 2002 SOPO report (DFO, 2003) describes anomalously warm waters in the subarctic Northeast Pacific and the shallowest mixed layer on record at that time.

This period coincides with the onset of significant changes in temporal and spatial trends of SST and chlorophyll (Figure 9.4) and in many of the *in situ* parameters included in this assessment (Figure 9.6).

The warmer conditions of the western North Pacific noted in this report have also been studied by other authors. For example, Park *et al*. (2012) reported that the western boundary of the subtropical North Pacific showed the greatest rate of warming of all oceans between 1981 and 2005. They attributed the temperature increase to rapid changes in both the Siberian High and Aleutian Low which, in turn, affected the subtropical gyre circulation of the North Pacific. Progressive warming in the Okhotsk Sea since the 1950s has also been observed (Nakanowatari *et al*., 2007). Cravatte *et al*. (2009) report on the consistent warming and freshening of the Western Pacific Warm Pool, an area that was observed to consistently increase in SST over the different time-windows examined here.

Variability in chlorophyll concentration across the North Pacific is largely connected to climate modes. For example, suppressed equatorial upwelling during El Niño events leads to a reduced nutrient supply, which affects primary production in the tropical Pacific and reduces chlorophyll concentrations. This also induces an asymmetric response of ocean chlorophyll to El Niño and La Niña in the central Pacific (Vantrepotte and Mélin, 2009; Park *et al*., 2011), a feature that can be seen in the data presented here. The SOPO report for 2006 (DFO, 2007) describes the onset of La Niña conditions and, at that time, the largest phytoplankton (coccolithophore) bloom ever recorded off Vancouver Island on the Canadian west coast. This period is encompassed by the 10-year IGMETS time-window (2003–2012), during which the percentage surface area of the North Pacific in which chlorophyll increased was greater than for other time-windows (Table 9.2), which suggests a slowing of the long-term downward trend in the open ocean. This was also the period during which the greatest number of *in situ* time series showed an increase in phytoplankton biomass (Figure 9.6b). The normally dominant PDO climate pattern shifted abruptly to its negative phase in 2007, coinciding with La Niña conditions and ushering in an unusually cool 5-year period (2008–2012).

The general decrease in surface chlorophyll noted here in the open North Pacific, as determined by satellite observations, is consistent with observations made by Polovina *et al*. (2008) and Signorini *et al*. (2015), who report on the expansion of low surface chlorophyll areas in the subtropical North Pacific from 1998 to 2006 and from 1998 to 2013, respectively, accompanied by significant increases in average sea surface temperature. This is also consistent with the reported increase in stratification in both subtropical oceanic and subarctic coastal waters. In the coastal eastern and western North Pacific, as well as near the western tropical Pacific, the higher chlorophyll concentrations that have been observed over the past 15 years have been linked to changes in nitrate concentrations and variation in the PDO (Rykaczewski and Dunne, 2010; Chiba *et al*., 2012). While some models project an increase in size of the Western Pacific Warm Pool (Matear *et al*., 2015), there may not be a significant change in primary productivity in the area despite the continued temperature increase.

Climate modes also impact the ecological variability of the North Pacific (Doney *et al*., 2012; Litzow and Mueter, 2014). For example, in the eastern North Pacific, zooplankton communities north and south of the southern California Bight have opposite trends following the shift from El Niño to La Niña in 1998 (McKinnell and Dagg, 2010), signifying a major geographical shift in patterns of lower trophic level productivity in response to climate change. This inverse relationship appears to be captured in the *in situ* zooplankton data for the 10-year time-window presented in this report (Figure 9.5d), further illustrating the coherence between this assessment and previously published reports on changing conditions in the North Pacific. The second North Pacific Ecosystem Status Report (McKinnell and Dagg, 2010) also describes 2003–2008 as a period of enhanced climatic and ecological variability, particularly in the eastern North Pacific where extreme values in some time series were observed. Similarly, Canadian SOPO reports (DFO, 2005–2007) document unusually warm conditions from 2004 to 2006, accompanied by an overall decrease in zooplankton and a shift to warm-water species along the Canadian west coast. These observations are consistent

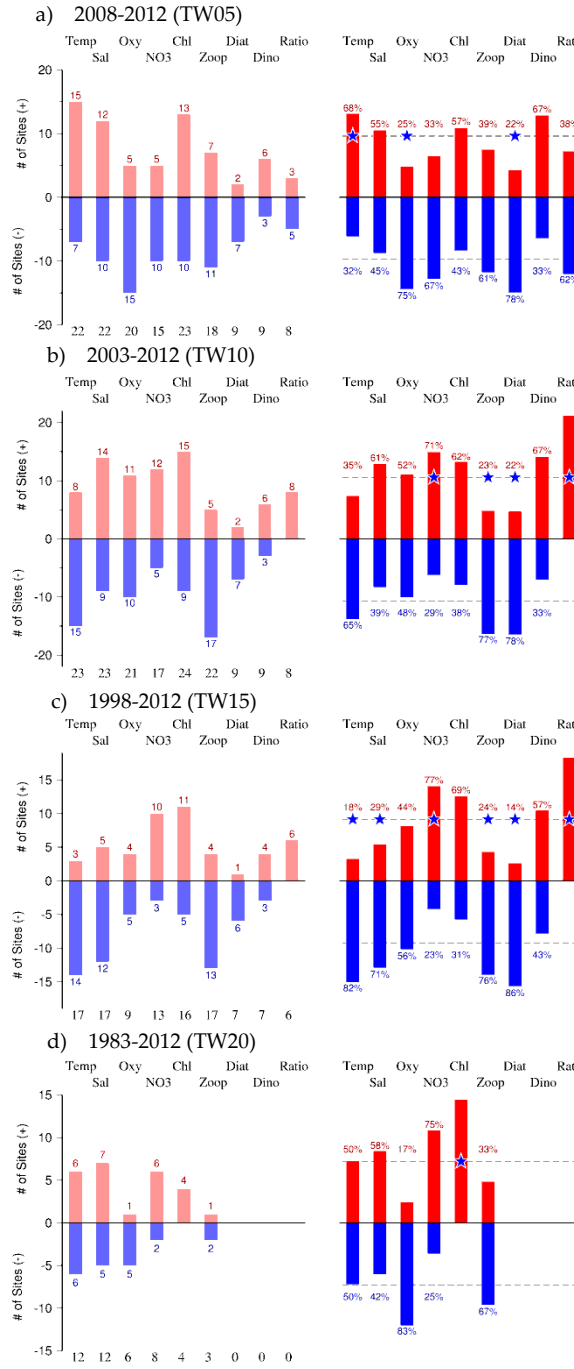

Figure 9.7. Absolute (left) and relative (%, right) frequency of positive and negative trends in selected variables from *in situ* time series in the North Pacific region computed for the 5-, 10-, 15-, and 30-year IGMETS time-windows. The 50% relative frequency is indicated by dashed lines in the left panels. A star symbol on the dashed line indicates a statistically significant difference ($p < 0.05$) from 50% positive/negative correlations. See "Methods" chapter for a complete description and methodology used.

Figure 9.6. Absolute (left) and relative (%, right) frequency of positive and negative correlations between selected *in situ* North Pacific time-series variables and corresponding gridded sea surface temperature (SST) for the 5-, 10-, 15-, and 30-year IGMETS time-windows. The 50% relative frequency is indicated by dashed lines in the left panels. A star symbol on the dashed line indicates a statistically significant difference ($p < 0.05$) from 50% positive/negative correlations. See "Methods" chapter for a complete description and methodology used.

with what was found for the time-window 2003–2010 in this assessment. From 2007 onwards, however, northern species of zooplankton once again predominated in western Canadian coastal waters (DFO, 2008–2011), illustrating the dynamic relationship between SST and the distribution of cold- and warm-water species.

The decrease in surface salinity of the northern and western North Pacific, as observed in this assessment (Figure 9.5g), has been attributed to changes in precipitation, evaporation, and sea ice. For example, Ohshima *et al*. (2014) attribute most of the freshening of the Okhotsk Sea to reduced sea ice production, with minor influences from variations in precipitation and evaporation over the region. Similarly, Hosoda *et al*. (2009) suggest that variations in precipitation and evaporation are the drivers behind the freshening of the northern North Pacific. The second North Pacific Ecosystem Status Report also describes long-term downward trends in surface oxygen and phosphate in the Oyashio Current that slowed after 1998 and show decadal variability linked to the PDO.

9.5 Conclusions

The North Pacific has undergone significant changes in ocean climate during the past three decades. Based on satellite SST measurements, > 75% (64% at $p < 0.05$) of its surface area has undergone significant warming since 1983. The patterns of change suggest that the PDO has been the dominant mode of climate variability in the North Pacific between 1983 and 2012. It is interesting to note that the subarctic Northeast Pacific has experienced little or no overall warming during this period, due to the dominance of a positive PDO prior to 1997 and negative PDO after 1998. However, marked variability in SST has been observed, with episodes of warming in 2002, 2004, and 2010 interspersed with periods of cooling, particularly since 2008 due to the combined effects of La Niña and a negative, cooling PDO phase. These changes and the resulting variability in key ocean parameters are captured in the IGMETS dataset and confirmed by other assessments of ocean conditions in the North Pacific.

Long-term time series in the central, subarctic northeast, and western North Pacific show an increase in phytoplankton biomass during the past 30 years. However, satellite observations suggest that over 65% of the surface of the North Pacific has experienced a decline in chlorophyll concentration since 1998. Available time-

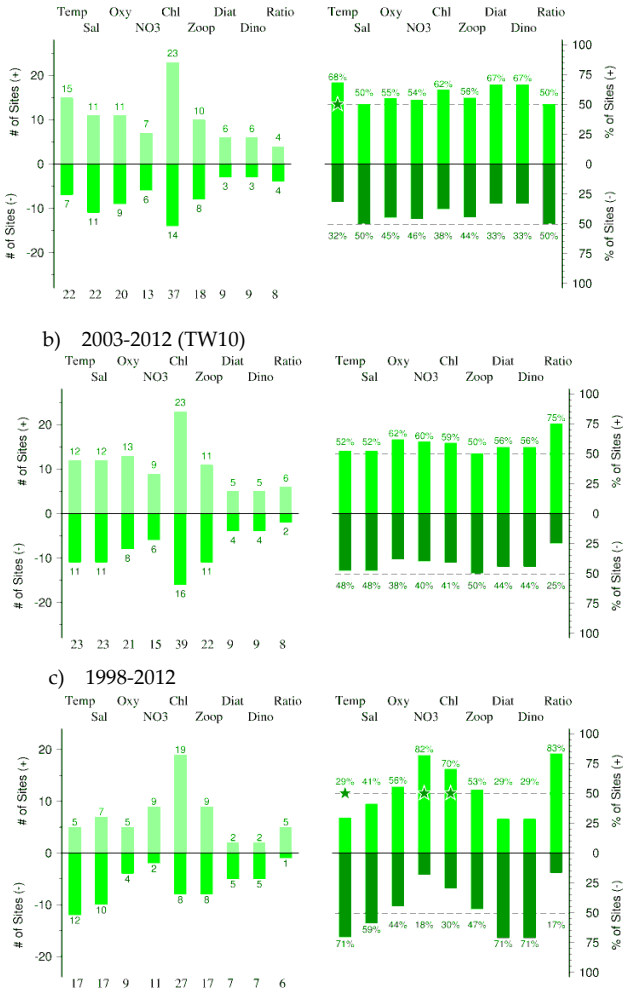

Figure 9.8. Absolute (left) and relative (%, right) frequency of positive and negative correlations between selected *in situ* North Pacific time series variables and corresponding gridded satellite chlorophyll for the 5-, 10-, and 15-year IGMETS time-windows. The 50% relative frequency is indicated by dashed lines in the left panels. A star symbol on the dashed line indicates a statistically significant difference ($p < 0.05$) from 50% positive/negative correlations. See "Methods" chapter for a complete description and methodology used.

series show an increase in zooplankton biomass in the waters off Hawaii, southern Vancouver Island, and the western United States during the last 15 years, but an overall decrease at most other locations, with no significant correlation between zooplankton biomass and chlorophyll. Nutrients, salinity, and dissolved oxygen at the ocean surface appear to be negatively correlated with SST across the North Pacific. Maintaining and, where possible, increasing the number of time series in this region would enhance our ability to identify and assess the impacts of long- and short-term climate change on North Pacific marine ecosystems.

Table 9.3. Regional listing of participating time series for the IGMETS North Pacific. Participating countries: Canada (ca), Colombia (co), China/Hong Kong (hk), Japan (jp), Republic of Korea (kr), Mexico (mx), United Kingdom (uk), and United States (us). Year-spans in red text indicate time series of unknown or discontinued status. IGMETS-IDs in red text indicate time series without a description entry in the Annex A7.

No.	IGMETS-ID	Site or programme name	Year-span	T	S	Oxy	Ntr	Chl	Mic	Phy	Zoo
1	ca-50301	Northern Vancouver Island – Offshore *(Canadian Pacific Coast)*	1983–present	-	-	-	-	-	-	-	X
2	ca-50302	Southern Vancouver Island – Offshore *(Canadian Pacific Coast)*	1979–present	-	-	-	-	-	-	-	X
3	ca-50901	Line P – P26 – OWS Papa *(Northeast North Pacific)*	1956–present	X	X	X	X	X	-	-	X
4	ca-50902	Line P – P20 *(Northeast North Pacific)*	1968–present	X	X	X	X	X	-	-	X
5	ca-50903	Line P – P16 *(Northeast North Pacific)*	1968–present	X	X	X	X	X	-	-	X
6	ca-50904	Line P – P12 *(Northeast North Pacific)*	1968–present	X	X	X	X	X	-	-	X
7	ca-50905	Line P – P08 *(Northeast North Pacific)*	1968–present	X	X	X	X	X	-	-	X
8	ca-50906	Line P – P04 *(Northeast North Pacific)*	1968–present	X	X	X	X	X	-	-	X
9	co-30110	REDCAM Department of Cauca *(Colombia Coastline)*	2002–present	X	X	X	-	-	-	-	-
10	co-30111	REDCAM Department of Choco *(Colombia Coastline)*	2002–present	X	X	X	-	-	-	-	-
11	co-30112	REDCAM Department of Narino *(Colombia Coastline)*	2002–present	X	X	X	-	-	-	-	-
12	co-30113	REDCAM Department of Valle del Cauca *(Colombia Coastline)*	2002–present	X	X	X	-	-	-	-	-
13	hk-30101	Hong Kong EPD Marine Water Quality Monitoring *(Hong Kong)*	1991–present	X	X	X	X	X	-	X	-
14	jp-30104	PM Line *(Japan Sea)*	1972–2002 (?)	-	-	-	-	-	-	-	X
15	jp-30101	Kuroshio Current *(Western North Pacific)*	1951–2002 (?)	X	-	-	-	-	-	-	X
16	jp-30102	Oyashio Current *(Western North Pacific)*	1951–2004 (?)	X	-	-	-	-	-	-	X
17	jp-30103	Oyashio–Kuroshio Transition *(Western North Pacific)*	1951–2004 (?)	X	-	-	-	-	-	-	X
18	jp-30201	Bering Sea – HUFO *(Bering Sea)*	1955–2006 (?)	-	-	-	-	-	-	-	X
19	jp-30202	Central North Pacific – HUFO *(North Pacific)*	1979–2000 (?)	-	-	-	-	-	-	-	X

No.	IGMETS-ID	Site or programme name	Year-span	T	S	Oxy	Ntr	Chl	Mic	Phy	Zoo
20	jp-30401	JMA East China Sea *(East China Sea)*	1965–present	X	X	X	X	-	-	-	-
21	jp-30402	JMA Japan Sea *(Japan Sea)*	1964–present	X	X	X	X	X	-	-	-
22	jp-30403	JMA Philippine Sea *(Philippine Sea)*	1965–present	X	X	X	X	X	-	-	-
23	jp-30404	JMA Southeast Hokkaido *(Northwest North Pacific)*	1965–present	X	X	X	X	X	-	-	-
24	jp-30405	JMA 137E Transect *(Lower Philippine Sea)*	1970–present	X	X	X	X	-	-	-	-
25	kr-30103	Korea East *(Japan Sea)*	1965–2006 (?)	-	-	-	-	-	-	-	X
26	kr-30104	Northeast Korea – Russian Sampling *(Japan Sea)*	1988–2007 (?)	-	-	-	-	-	-	-	X
27	kr-30102	Korea South *(East China Sea)*	1965–2006 (?)	-	-	-	-	-	-	-	X
28	kr-30101	Korea West *(Yellow Sea)*	1965–2006 (?)	-	-	-	-	-	-	-	X
29	mx-30101	IMECOCAL Northern Baja – NB *(Southeastern North Pacific)*	1998–present	-	-	-	-	-	-	-	X
30	mx-30102	IMECOCAL Southern Baja – SB *(Southeastern North Pacific)*	1998–present	-	-	-	-	-	-	-	X
31	uk-40201	Pacific CPR – Southern Bering Sea *(Northeastern North Pacific)*	2000–present	-	-	-	-	X	-	X	X
32	uk-40202	Pacific CPR – Aleutian Shelf *(Northeastern North Pacific)*	2000–present	-	-	-	-	X	-	X	X
33	uk-40203	Pacific CPR – Western Gulf of Alaska *(Northeastern North Pacific)*	2000–present	-	-	-	-	X	-	X	X
34	uk-40204	Pacific CPR – Alaskan Shelf *(Northeastern North Pacific)*	2004–present	-	-	-	-	X	-	X	X
35	uk-40205	Pacific CPR – Cook Inlet *(Northeastern North Pacific)*	2004–present	-	-	-	-	X	-	X	X
36	uk-40206	Pacific CPR – Northern Gulf of Alaska *(Northeastern North Pacific)*	1997–present	-	-	-	-	X	-	X	X
37	uk-40207	Pacific CPR – Offshore BC *(Northeastern North Pacific)*	1997–present	-	-	-	-	X	-	X	X
38	uk-40208	Pacific CPR – BC Shelf *(Northeastern North Pacific)*	2000–present	-	-	-	-	X	-	X	X
39	us-10201	Hawaii Ocean Time series – HOT *(Central North Pacific)*	1988–present	X	X	X	X	X	X	-	X

No.	IGMETS-ID	Site or programme name	Year-span	T	S	Oxy	Ntr	Chl	Mic	Phy	Zoo
40	us-10301	USC WIES San Pedro Ocean Time series – SPOT *(Eastern North Pacific)*	2000–present	X	X	X	X	X	-	-	-
41	us-30401	Central Bay *(San Francisco Bay)*	1978–present	X	X	X	X	X	X	X	-
42	us-50301	CalCOFI California Current region – CC *(California Current)*	1951–present	-	-	-	-	-	-	-	X
43	us-50302	CalCOFI Southern California region – SC *(Southern California Current)*	1951–present	-	-	-	-	-	-	-	X
44	us-50401	Western Kodiak Island – EcoFOCI *(Gulf of Alaska)*	1981–present	-	-	-	-	-	-	-	X
45	us-50501	Newport Line NH-5 *(Newport-Oregon)*	1969–present	X	X	-	X	X	-	-	X
46	us-50601	EMA-1: Eastern Bering Sea – East *(Southeastern Bering Shelf)*	1999–present	X	X	X	X	X	-	-	X
47	us-50602	EMA-2: Eastern Bering Sea – West *(Southwestern Bering Shelf)*	2002–present	X	X	X	X	X	-	-	X
48	us-50603	EMA-3: Northern Bering Sea *(Northern Bering Sea)*	2002–present	X	X	X	X	X	-	-	X
49	us-60106	NERRS Elkhorn Slough *(Northeastern North Pacific)*	2001–present	X	X	X	X	X	-	-	-
50	us-60113	NERRS Kachemak Bay *(Northeastern North Pacific)*	2003–present	X	X	X	X	X	-	-	-
51	us-60120	NERRS Padilla Bay *(Northeastern North Pacific)*	2009–present	X	X	X	X	X	-	-	-
52	us-60123	NERRS San Francisco Bay *(Northeastern North Pacific)*	2008–present	X	X	X	X	X	-	-	-
53	us-60124	NERRS South Slough *(Northeastern North Pacific)*	2002–present	X	X	X	X	X	-	-	-
54	us-60125	NERRS Tijuana River *(Northeastern North Pacific)*	2004–present	X	X	X	X	X	-	-	-

9.6 References

Batten, S. D., and Crawford, W. R. 2005. The influence of coastal origin eddies on oceanic plankton distribution in the eastern Gulf of Alaska. Deep-Sea Research II, 52: 991–1009.

Bowditch, N. 2002. American Practical Navigator: An Epitome of Navigation and Nautical Astronomy. Publication No. 9. National Imagery and Mapping Agency, Bethesda, MD. 879 pp.

Chandler, P. C., King, S. A., and Perry, R. I. (Eds). 2015. State of the physical, biological and selected fishery resources of Pacific Canadian marine ecosystems in 2014. Canadian Technical Report of Fisheries and Aquatic Science, 3131. 211 pp.

Chiba, S., Batten, S., Sasaoka, K., Sasai, Y., and Sugisaki, K. 2012. Influence of the Pacific Decadal Oscillation on phytoplankton phenology and community structure in the western North Pacific. Geophysical Research Letters, 39: L15603, doi:10.1029/2012GL052912.

Cloern, J. E., Hieb, K. A., Jacobsen, T., Sanso, B., Di Lorenzo, E., Stacey, M. T., Largier, J. L., *et al*. 2010. Biological communities in San Francisco Bay track large-scale climate forcing over the North Pacific. Geophysical Research Letters, 37: L21602, http://dx.doi.org/10.1029/2010GL044774.

Cravatte, S., Delcroix, T., Zhang, D., McPhaden, M. J., and Leloup, J. 2009. Observed freshening and warming of the western Pacific warm pool. Climate Dynamics, 33: 565–589, doi:10.1007/s00382-009-0526-7.

DFO. 2000. http://waves-vagues.dfo-mpo.gc.ca/Library/324619.pdf.

DFO. 2001. http://waves-vagues.dfo-mpo.gc.ca/Library/324620.pdf.

DFO. 2002. http://waves-vagues.dfo-mpo.gc.ca/Library/265807.pdf.

DFO. 2003. http://waves-vagues.dfo-mpo.gc.ca/Library/324622.pdf.

DFO. 2005. http://waves-vagues.dfo-mpo.gc.ca/Library/324624.pdf.

DFO. 2006. http://www.dfo-mpo.gc.ca/Library/324625.pdf.

DFO. 2007. http://www.dfo-mpo.gc.ca/Library/328475.pdf.

DFO. 2008. http://www.dfo-mpo.gc.ca/csas-sccs/publications/SAR-AS/2008/SAR-AS2008_028_e.pdf.

DFO. 2009. http://www.dfo-mpo.gc.ca/csas-sccs/publications/SAR-AS/2009/2009_030_e.pdf.

DFO. 2010. http://www.dfo-mpo.gc.ca/csas-sccs/publications/sar-as/2010/2010_034_e.pdf.

DFO. 2011. http://www.dfo-mpo.gc.ca/csas-sccs/Publications/SAR-AS/2011/2011_032-eng.pdf.

Di Lorenzo, E., Combes, V., Keister, J. E., Strub, P. T., Thomas, A. C., Franks, P. J. S., Ohman, M. D., *et al*. 2013. Synthesis of Pacific Ocean climate and ecosystem dynamics. Oceanography, 26(4): 69–81.

Di Lorenzo, E., Fiechter, J., Schneider, N., Bracco, A., Miller, A. J., Franks, P. J. S., Bograd, S. ., *et al*. 2009. Nutrient and salinity decadal variations in the central and eastern North Pacific. Geophysical Research Letters, 36: L14601, doi:10.1029/2009GL038261.

Di Lorenzo, E., Schneider, N., Cobb, K. M., Franks, P. J. S., Chhak, K., Miller, A. J., McWilliams, J. C., *et al*. 2008. North Pacific Gyre Oscillation links ocean climate and ecosystem change. Geophysical Research Letters, 35: L08607, doi:10.1029/2007GL032838.

Doney, S. C., Ruckelshaus, M., Duffy, J. E., Barry, J. P., Chan, F., English, C. A., Galindo, H. M., *et al*. 2012. Climate change impacts on marine ecosystems. Annual Review of Marine Science, 4: 11–37, doi:10.1146/annurev-marine-041911-111611.

Dutkiewicz, S., Follows, M., Marshall, J., and Gregg, W. W. 2001. Interannual variability of phytoplankton abundances in the North Atlantic. Deep-Sea Research II, 48: 2323–2344.

Eakins, B. W., and Sharman, F. 2010. Volumes of the World's Oceans from ETOPO1. NOAA National Geophysical Data Center, Boulder, CO.

Feely, R. A., Sabine, C. L., Hernandez-Ayon, J. M., Ianson, D., and Hales, B. 2008. Evidence for upwelling of corrosive "acidified" water onto the Continental Shelf. Science, 320: 1490–1492.

Haigh, R., Ianson, D., Holt, C. A., Neate, H. E., and Edwards, A. M. 2015. Effects of ocean acidification on temperate coastal marine ecosystems and fisheries in the Northeast Pacific. PLoS One, 10(2): e0117533, https://doi:10.1371/journal.pone.0117533.

Hosoda, S., Suga, T., Shikama, N., and Mizuno, K. 2009. Global surface layer salinity change detected by Argo and its implication for hydrological cycle intensification. Journal of Oceanography, 65: 579–586.

Johnson, K. W., Miller, L. A., Sutherland, N. E., and Wong, C. S. 2005. Iron transport by mesoscale Haida eddies in the Gulf of Alaska. Deep-Sea Research II, 52: 933–953.

Karl, D. M. 1999. A sea of change: biogeochemical variability in the North Pacific Subtropical Gyre. Ecosystems, 2(3): 181–214.

Litzow, M. A., and Mueter, F. J. 2014. Assessing the ecological importance of climate regime shifts: An approach from the North Pacific Ocean. Progress in Oceanography, 120: 110–119, http://dx.doi.org/10.1016/j.pocean.2013.08.003.

Longhurst, A. 2007. Ecological Geography of the Sea, 2nd edn. Elsevier, San Diego. 398 pp.

Mantua, J. N., Hare, S. R., Zhang, Y., Wallace, J. M., and Francis, R. C. 1997. A Pacific interdecadal climate oscillation with impacts on salmon production. Bulletin of the American Meteorological Society, 78: 1069–1080.

Matear, R. J., Chamberlain, M. A, Sun, C., and Feng, M. 2015. Climate change projection for the western tropical Pacific Ocean using a high-resolution ocean model: Implications for tuna fisheries. Deep-Sea Research II: Topical Studies in Oceanography, 113: 22–46, http://dx.doi.org/10.1016/j.dsr2.2014.07.003.

McKinnell, S. M., and Dagg, M. J. (Eds). 2010. Marine Ecosystems of the North Pacific Ocean, 2003-2008. PICES Special Publication, 4. 393 pp.

Minobe, S., Kuwano-Yoshida, A., Komori, N., Xie, S-P., and Small, R. J. 2008. Influence of the Gulf Stream on the troposphere. Nature, 452: 206–209.

Nakanowatari, T., Ohshima, K. I., and Wakatsuchi, M. 2007. Warming and oxygen decrease of intermediate water in the northwestern North Pacific, originating from the Sea of Okhotsk, 1955–2004. Geophysical Research Letters, 34: L04602, doi:10.1029/2006GL028243.

Ohshima, K. I., Nakanowatari, T., Riser, S., Volkov, Y., and Wakatsuchi, M. 2014. Freshening and dense shelf water reduction in the Okhotsk Sea linked with sea ice decline. Progress in Oceanography, 126: 71–79, http://dx.doi.org/10.1016/j.pocean.2014.04.020.

Park, J-Y., Kug, J-S. F., Park, J., Yeh, S-W., and Jang, C. J. 2011. Variability of chlorophyll associated with El Niño–Southern Oscillation and its possible biological feedback in the equatorial Pacific. Journal of Geophysical Research, 116: C10001, doi:10.1029/2011JC007056.

Park, J-Y., Yoon, J-H , Youn, Y-H., and Vivier, F. 2012. Recent warming in the Western North Pacific in relation to rapid changes in the atmospheric circulation of the Siberian High and Aleutian Low systems. Journal of Climate, 25: 3476–3493, doi:http://dx.doi.org/10.1175/2011JCLI4142.1.

Perry, R. I., and Masson, D. 2013. An integrated analysis of the marine social-ecological system of the Strait of Georgia, Canada over the past four decades, and development of a regime shift index. Progress in Oceanography, 115: 14–27.

PICES. 2004. Marine Ecosystems of the North Pacific. PICES Special Publication, 1. 280 pp.

Polovina, J. J., Howell, E. A., and Abecassis, M. 2008. Ocean's least productive waters are expanding. Geophysical Research Letters 35: L03618, doi:10.1029/2007GL031745.

Rykaczewski, R. R., and Dunne, J. P. 2010. Enhanced nutrient supply to the California Current Ecosystem with global warming and increased stratification in an earth system model. Geophysical Research Letters, 37: L21606, doi: 10.1029/2010GL045019.

Signorini, S. R., Franz, B. A., and McClain, C. R. 2015. Chlorophyll variability in the oligotrophic gyres: mechanisms, seasonality and trends. Frontiers in Marine Science, 2(1): doi: 10.3389/fmars.2015.00001.

Trenberth, K. E., and Hurrell, J. W. 1994. Decadal atmosphere-ocean variations in the Pacific. Climate Dynamics, 9: 303–319.

Vantrepotte, V., and Mélin, F. 2009. Temporal variability of 10-year global SeaWiFS time series of phytoplankton chlorophyll *a* concentration. ICES Journal of Marine Science, 66(7): 1547-1556, doi:https://doi.org/10.1093/icesjms/fsp107.

Wallace, J. M., and Gutzler, D. S. 1981. Teleconnections in the Geopotential Height Field during the Northern Hemisphere Winter. Monthly Weather Review, 109: 784–812.

Wu, L., Cai, W., Zhang, L., Nakamura, H., Timmermann, A., Joyce, T., McPhaden, M. J., *et al*. 2012. Enhanced warming over the global subtropical western boundary currents. Nature Climate Change, 2: 161–166.

Zenk, W. 2001. Abyssal currents. *In* Encyclopedia of Ocean Sciences, pp. 12–28. Ed. by J. H. Steele, K. K. Turekian, and S. A. Thorpe. Elsevier. 3399 pp.

Zhang, Y., Wallace, J. M., and Battisti, D. S. 1997. ENSO-like interdecadal variability: 1900-93. Journal of Climate, 10: 1004–1020.